Assessment of the porosity effect on tensile behavior of Ti-6Al-4V samples produced by Laser Engineered Net Shaping technology

Journal:	*Part C: Journal of Mechanical Engineering Science*
Manuscript ID	JMES-18-0581.R1
Manuscript Type:	Mechanical Characterization of Parts Fabricated by Additive Manufacturing
Date Submitted by the Author:	n/a
Complete List of Authors:	Razavi, Seyed Mohammad Javad; NTNU Fakultet for ingeniorvitenskap og teknologi Trondheim Bordonaro, G.G. Ferro, P.; Univ Padua torgersen, j Berto, Prof. Filippo; NTNU Fakultet for ingeniorvitenskap og teknologi Trondheim,
Keywords:	Additive Manufacturing, Direct Energy Deposition, Laser Engineered Net Shaping, Porosity, Titanium Alloy
Abstract:	Microstructural characteristics of additively manufactured Ti-6Al-4V specimens are analyzed in this study. Laser Engineered Net Shaping technology (LENS), a Direct Energy Deposition (DED) additive manufacturing (AM) process, is used to fabricate specimens. Effects of process parameters including machine head laser power, head write speed, layer height, hatch spacing, and powder flow rate on the morphological features of the material are investigated. A first batch of samples is built with a combination of parameters leading to full density metal parts across each layer and near-zero defects likewise more conventional process techniques (i.e., wrought and casting). A second batch of samples is built with a set of processing parameters aimed to induce defects within the parts like voids and porosity. Samples from both batches were stress-relieved in order to remove internal residual stresses generated by the additive manufacturing process. Optical Microscopy (OM), Scanning Electron Microscopy (SEM) and X-ray diffraction (XRD) were used to characterize the microstructure of all samples. Tensile properties were measured after the stress-relief heat treatment. It was found that LENS parts are strongly sensitive to variations of building process parameters. Different structure morphologies were observed for different incident energies and cooling rates due to the combination of head write speed and laser power. The grain size distribution and shape are influenced by the powder flow rate resulting in either equiaxed or columnar grain microstructures with the formation of defects such as pores, unmelted regions, and gas entrapment. Non-porous specimens exhibit tensile and ductility properties comparable with the wrought counterpart, but porous specimens were found to show a reduced strength and ductility.

Original article (Special Issue: Mechanical Characterization of Parts Fabricated by Additive Manufacturing)

Porosity effect on tensile behavior of Ti-6Al-4V samples produced by Laser Engineered Net Shaping technology

S.M.J. Razavi[1], G.G. Bordonaro[2], P. Ferro[3], J. Torgersen[1], F. Berto[1*]

[1] Department of Mechanical and Industrial Engineering, Norwegian University of Science and Technology (NTNU), Richard Birkelands vei 2b, 7491, Trondheim, Norway.

[2] Institute for Mechanical Engineering and Materials Technology, Galleria 2, Via Cantonale 2c, University of Applied Sciences of Southern Switzerland, CH-6928 Manno, Switzerland.

[3] Department of Engineering and Management, University of Padova, Stradella San Nicola 3, 36100 Vicenza, Italy.

*Corresponding author (Filippo Berto): Tel.: +47-73594129; E-mail address: Filippo.berto@ntnu.no

Abstract

Microstructural characteristics of additively manufactured Ti-6Al-4V specimens are analyzed in this study. Laser Engineered Net Shaping technology (LENS), a Direct Energy Deposition (DED) additive manufacturing (AM) process, is used to fabricate specimens. Effects of process parameters including machine head laser power, head write speed, layer height, hatch spacing, and powder flow rate on the morphological features of the material are investigated. A first batch of samples is built with a combination of parameters leading to full density metal parts across each layer and near-zero defects likewise more conventional process techniques (i.e., wrought and casting). A second batch of samples is built with a set of processing parameters aimed to induce defects within the parts like voids and porosity. Samples from both batches were stress-relieved in order to remove internal residual stresses generated by the additive manufacturing process. Optical Microscopy (OM), Scanning Electron Microscopy (SEM) and X-ray diffraction (XRD) were used to characterize the microstructure of all samples. Tensile properties were measured after the stress-relief heat treatment. It was found that LENS parts are strongly sensitive to variations of building process parameters. Different structure morphologies were observed for different incident energies and cooling rates due to the combination of laser power and head write speed. The grain size distribution and shape are influenced by the powder flow rate resulting in either equiaxed or columnar grain microstructures with the development of material defects such as pores, gas entrapment and lack of fusion. Non-porous specimens revealed comparable tensile and ductility properties with the wrought counterpart, however, porous specimens were found to have a reduced strength and ductility.

Keywords

Additive Manufacturing; Direct Energy Deposition; Laser Engineered Net Shaping; Porosity; Titanium Alloy.

1. Introduction

Additive manufacturing (AM) technology is rapidly developing in many industrial fields, such as automotive, aerospace, oil and gas, and biomedical. The possibility to reduce the design to manufacture time and fabricate structural components with precise and accurate geometry, makes it an attractive technique to be implemented in industrial processes. However, several studies show that the quality and performance of AM materials are largely affected by AM processing parameters in terms of internal unwanted defects, porosity, and microstructure. AM materials exhibit anisotropic properties due to large inhomogeneous void distributions, unmelted regions of powder, layers deposition directions. The challenge, thus, is to develop a deeper understanding of how microstructure and mechanical behaviour of AM products relate to processing parameters before these materials can be safely employed in actual and even critical load-bearing applications. Hofmeister et al.[1] performed a sensitivity analysis of the metallographic features variations depending upon solidification and cooling rates for directly energy deposited samples made of 316 stainless steel material. The microstructural scale was found to be more sensitive to variations in the vertical direction (height z) than to changes in laser power and transverse velocity. Carlton et al.[2] measured three-dimensional pore

morphology and volume distribution in stainless steel at the micrometre length scale using a Synchrotron Radiation micro-Tomography while applying tensile tests on stainless steel samples fabricated via Selective Laser Melting (SLM) manufacturing process to track damage evolution. Stucker et al.[3] analysed hardness, microstructure, and wear trends of CoCrMo alloy samples produced by Direct Energy Deposition process (DED) and found that they are harder and less resistant to abrasive wear than wrought alloys. Prabhu et al.[4] evaluated fatigue properties of as-deposited DED parts and "repair condition" deposits. The effects of different microstructures on fatigue life were assessed with respect to cast and wrought materials. Results of this study confirmed the potential of DED deposits to have fatigue life similar to wrought materials without the requirement of Hot Isostatic Pressing (HIP).

DED is an additive manufacturing process that includes the following commonly used printing technologies: Laser Engineered Net Shaping (LENS), Direct Metal Deposition (DMD), Directed Light Fabrication (DLF) and 3D laser cladding. It is commonly used to repair or add additional material to existing components.[5] A typical configuration of a DED machine incorporates one or multiple nozzles mounted on a multi axes arm. The material is deposited and melted upon deposition with a laser or electron beam onto a specified surface where solidifies in a controlled-atmosphere chamber with reduced oxygen levels. Nozzles can move in multiple directions such that the material is deposited from any angle through the multiple axes machine. The process can be employed for fabrication of polymers and ceramics; however, it is typically used with metals, in the form of either powder or wire. Although wire is less accurate than powder because of the pre-formed shape, it is more efficient in terms of material consumption[5] because only the

required amount of material is used. Compared to a fixed, vertical deposition machine, the multiple axes feed head does not change the flow rate of the material.[5] The final grain microstructure of the deposited material is typically uniformly distributed but alternating due to the overlapping of material which can cause re-melting to occur despite high cooling rates (between 1000 and 5000^{o}C/s).

In this work, LENS is used to fabricate Ti-6Al-4V specimens. Effects of different process parameters including machine head laser power, head write speed, layer height, hatch spacing, and powder flow rate on microstructural properties and porosity levels of the material are investigated. The microstructure is analysed in terms of grain morphology, size, and nature of phases. Tensile testing is also performed at room temperature to determine the mechanical properties of porous and non-porous specimens. The fracture surface is examined to assess the effect of the microstructure on ductility and anisotropy characteristics. Titanium alloy is one of the most widely used materials for high end additively manufacturing applications due to its high strength and corrosion resistance at temperatures up to 773 K (500°C) in addition to low density and biocompatibility properties. LENS® technology[6] is a common type of DED process that uses multiple nozzles for the blown powder deposition. It is possible to regulate nozzles feed rate in order to induce different microstructural characteristics based on the chemical composition of the material. It provides a wide process window for the fabrication of large parts relative to other metal-based AM solutions. Due to high deposition rates, it provides excellent metallurgical bonding and material density, low distortion and minimal micro-cracking within the built part. It is indicated for repairing operations as well as conventional additive manufacturing applications. In contrast, the surface

roughness of the built component is not comparable with other additive manufacturing technologies, requiring additional finishing operations. Induced porosity in AM components can be used as a tool to control the location of failure initiation under static and cyclic loading. Additionally, due to higher biocompatibility of the porous materials, it is quite favourable for the components which are used in biomedical applications.

2. Experimental procedure and setup

2.1. Samples fabrication

LENS AM technique allows to fabricate metallic parts through a layer-by-layer sequential deposition of material. A laser beam is radiated by a moving laser head towards a focal point where the metallic powder is deposited through multiple nozzles to create a metal pool on a metallic solid substrate. The laser head moves over a track creating a molten line and the overlapping of these molten lines creates a single layer shape. The next layer is deposited following the same pattern by raising the deposition head upward by a layer thickness defined by the user. This process is repeated until the solid metallic part is built according to the CAD model of the desired product. The use of Argon prevents the machine chamber from oxidation during deposition ensuring an inert atmosphere (< 2ppm Oxygen).

An OPTOMEC LENS^{TM} 850-R machine is used to fabricate flat Ti-6Al-4V samples in batches of one sample per substrate (Ti-6Al-4V, 6 mm thick) and are deposited to a height of 81 mm. Spherical Ti-6Al-4V Grade 5 powder with a mesh size of -100/+325

(SAE AMS 4998C) is used for samples manufacturing. Two different sets of process parameters have been selected. The first set of processing parameters is aimed at minimizing interlayer porosity and obtaining full-dense specimens (non-porous specimens). The process parameters consisted of a laser power of 325 W, a head write speed of 25 in/min, a layer height of 0.02 in, a hatch spacing of 0.015 in, and a powder flow rate of 1.9 gr/min. These parameters were held constant until the first batch of samples was completely built. The second set of processing parameters was selected with the objective of inducing the formation of voids and porosities within the samples. Build and inspect method with various parameters combinations was performed before building the whole batch of porous specimens. The final set of additive manufacturing process parameters for the porous specimens is: laser power of 250 W, head write speed of 40 in/min, layer height of 0.02 in, hatch spacing of 0.03 in, and powder flow rate of 5.9 gr/min.

Samples were fabricated with a rectangular cross-section of 4×16 mm and a length of 81 mm deposited over a 6 mm thick substrate. Fig. 1 (a) shows the dimensioned drawing of the specimen and Fig. 1 (b) shows the as-built LENS Ti-6Al-4V specimen deposited on a substrate.

2.2. Heat treatment process

Due to presence of high temperature gradients and cooling rates during the fabrication operations, internal residual stresses are commonly induced within the DED parts. Hence, the LENS Ti-6Al-4V specimens were heat treated prior to mechanical testing. Stress

relief annealing was performed by inducing the samples in a preheated furnace at 600 °C (~1100 °F) for one hour followed by cooling at room temperature. Further studies on the effect of heat treatment and fabrication strategy on the residual stress level in AM Ti-6Al-4V components have been conducted in some recently published articles[7-9].

[insert Figure 1.]

2.3. Machining operations

After heat treating all LENS Ti-6Al-4V specimens, they were machined with the dimensions and configuration as shown Fig.2 according to ASTM E 606-92 standard resulting a mean surface roughness of 0.25 μm for all surfaces of the specimens. Five samples were produced for each set of materials.

[insert Figure 2.]

2.4. Metallographic specimen preparation

In order to reveal the pore size, distribution, and morphology, a series of metallographic specimens were prepared using conventional methods and examined using an Optical Microscope (OM) and Scanning electron microscope (SEM). Porosity distribution over a sample cross sectional area was measured to be in a range of 150 μm to 300 μm.

Samples were examined using X-ray diffraction and etched in an etching solution containing 50 ml distilled water, 25 ml HNO_3 and 5 ml HF for microstructural investigation using OM and SEM.

2.5. Tensile tests procedure

Tensile tests were performed at room temperature using an Instron 5969 testing machine (Massachusetts-United States) universal testing machine with a 50 kN load cell to obtain the load-displacement curves of the fabricated samples. A strain rate of 1.0×10^{-4} s^{-1} was used to conduct static tests under strain control mode. Afterwards, the failure surfaces were examined using SEM.

3. Results and Discussion

3.1. Porosity and surface morphology

Before sectioning the samples for optical microscope (OM) investigations, X-Ray inspections were carried out both on porous and non-porous specimens by using the X-Ray testing cabinet Bosello SRE 80 MAN.

Fig. 3 shows X-Ray photographs of porous and non-porous samples. It is clearly shown the pattern of the porosity induced by the LENS process and the complete absence of porosity in the non-porous specimen. The induced pores are uniformly distributed in each building layer along the vertical building direction. The morphology of the pores is either

near-spherical with ridges inside or flat irregular-shaped with sharp angles. The first type of pores appears to mainly form due to gas entrapment at the interface between two adjacent layers and show a size ranging from 50 µm and 100 µm in diameter. Incomplete re-melting and lack of fusion[10] resulted the second type of defects with a size range of 100 – 200 µm.

[insert Figure 3.]

3.2. Microstructure

Considering the OM pictures, the alpha prime and acicular alpha structures of titanium alloy appear to be white after etching whereas intergranular beta structure and beta grains have a darker color. Similar to other researches dealing with Ti-6Al-4V specimens produced by AM techniques[11-17], a columnar grain structure is observed as a result of the epitaxial growth caused by the sequential layers deposition (Figs. 4a and 5a). These columnar grains grow over the layers of building and can reach a length of 3 mm and a width of 0.2-0.3 mm. Figs. 4 and 5 show the microstructure of the porous and non-porous specimens, respectively, at different magnifications.

[insert Figure 4.]

[insert Figure 5.]

The metal powder solidifies to form the β phase that subsequently transforms during

cooling. According to Figs. 4b and 5b, a martensitic microstructure with acicular α' grains is observed on heat treated samples with a higher magnification, which is a characteristic for LENS parts. For the mentioned materials, the anisotropic texture of grains is no more visible. This type of microstructure induced by the high cooling rate that characterizes the process, explains the low ductility of these specimens[15]. In their X-ray diffraction analyses on SLM Ti-6Al-4V samples, Qiu et al.[17] reported that no β peaks exists for both as-fabricated and stress-relieved (600 °C) samples. Moreover, they've reported a slight shift in the α-phase peaks to lower 2θ angles due to stress relief, suggesting that the α′-α transformation has occurred during stress relief. This phase transformation is supposed to be partially occurred also in the samples analyzed in this work during the stress-relief heat treatment. Finally, in Fig. 5a porosities, marked with red arrows, are clearly visible.

As a comparison with the AM microstructure, Fig. 6 shows the microstructure of the wrought Ti-6Al-4V alloy at different magnifications. In this case the microstructure is isotropic and consist of equiaxic alpha grains decorated with dark β phase.

[insert Figure 6.]

3.3. Tensile properties and fracture mechanism

Tensile testing was performed on both porous and non-porous samples and the typical stress-strain curves are illustrated in Fig. 7a. According to Fig. 7a, 0.2 % yield strength of 914 MPa and 960 MPa and ultimate tensile strength of 987 MPa and 1068 MPa were

obtained respectively for porous and non-porous samples. Elongation of porous and non-porous samples were about 1.95 % and 6.52 %, respectively.

Tensile behaviour of the wrought specimen is also shown in Fig. 7b for reference stating 0.2 % yield strength of 1062, ultimate tensile strength of 1089 MPa and elongation of 7.46 %.

As the local stress concentrators, porosities affect the overall behaviour of the printed part by reducing the ductility of the sample resulting the elongation at failure of the porous samples to be almost one third of the one obtained for the AM non-porous sample.

[insert Figure 7.]

Figure 8 show the SEM micrographs of the fracture surfaces of the wrought samples. The figure illustrates the occurrence of ductile/brittle fracture, with a predominance of a ductile fracture and the presence of ductile equiaxed dimples and cleavage facets. The wrought samples exhibited an irregular fracture surface related to the α phase.

Two types of fracture mechanisms namely ductile and brittle-like were observed in the SEM analyses. The high amount of plastic deformation results in ductile fracture shown in a grey colour surface. While, the movement of cracks involving very small plastic deformation resulting a brittle fracture. Cleavage fracture is indicated by brittle facets that reflect light.

The inner region of fracture surface was mainly dominated by the ductile mode of fracture (Fig. 8b and 8c) and characterised by microvoids and ductile dimples. While the surrounding area of fracture surface was characterised with considerable percentage of

cleavage with fewer dimples and higher cleavage facets. This type of failure is common among the ductile materials experiencing fibrous and shear failure mechanisms at the same time. Due to existence of maximum shear stress at 45°, the fracture surface is inclined in the boundaries of the fracture surface followed by fibrous ductile failure with 90° angle with respect to the loading direction in the centre of the cross section.

[insert Figure 8.]

The SEM micrographs of the fracture surfaces of AM non-porous samples are illustrated in Fig. 9. A combined ductile and brittle fracture, with a predominance of brittle fracture can be seen in Fig. 9. According to Fig. 9b, the microcavities are more elongated having cleavage areas, which may be related to the contribution of local shearing.

[insert Figure 9.]

Fig. 10 shows that fracture surfaces of the AM porous samples are rough and have deeper dimples (see Fig. 10b) in comparison with the non-porous specimens, proving the brittle behaviour of these samples. The presence of voids and lack of proper penetration during the manufacturing process resulted in incomplete fusion of the particles between the sintered layers. A predominance of brittle fracture occurred in the porous samples due to the existence of the voids making the microcracks to spread easier along the section.

In the porous samples with lower tensile strength and elongation at failure, large voids were identified as a result of lack of melt penetration. The voids produce local stress

concentration, which facilitates the propagation of cracks in AM porous samples. The destructive effect of the induced porosities can be in a higher level of importance when the component is loaded under cyclic loading. In this case, these stress raisers can significantly reduce the fatigue strength of the material[18].

[insert Figure 10.]

According to the results obtained in this study, the LENS additive manufacturing technique can be a substitute method for producing the metallic components. Comparing the experimental results of tensile testing of the wrought Ti-6Al-4V samples with the samples produced by LENS techniques revealed that comparable mechanical behaviour was obtained for AM produced samples. However, adequate fabrication parameters are required to obtain the proper mechanical behaviour of the fabricated samples. Dealing with the LENS porous samples, it was observed that although presence of the voids considerably reduced the ductility of the samples, however, the ultimate tensile strength of porous samples was almost identical with the non-porous samples produced by LENS.

4. Conclusions

The tensile behavior of Ti-6Al-4V specimens fabricated by LENS technology was assessed. Two series of tensile test samples with induced porosity and non-porous were printed using different process parameters. The size and distribution of voids in porous samples were evaluated using X-Ray photography and optical microscopy. The tensile

test results of the two types of LENS samples were compared with the wrought specimens. The fracture surface of failed samples was analyzed using SEM to classify the failure mechanisms. There is no statistically significant difference in tensile strength between the non-porous samples produced by LENS and the wrought samples. Although there was a considerable number of defects in the porous samples, they had an ultimate tensile strength of 987 MPa which is close to the values of 1068 MPa and 1089 MPa obtained for non-porous and wrought samples. However, the porous samples had considerably lower elongation at failure which was a results of stress raisers in the material, which facilitates the propagation of cracks in the sample. Fracture analysis of the porous samples indicated brittle fracture, and the non-porous samples exhibited mixed ductile/brittle fracture, with the predominance of brittle fracture in the presence of cleavage areas. The wrought samples exhibited a mixed ductile/brittle fracture with the predominance of ductile fracture.

Funding

This research did not receive any specific grant from funding agencies in the public, commercial, or not-for-profit sectors.

Declaration of Conflicting Interests

The Authors declare that there is no conflict of interest.

References

1. Hofmeister W and Griffith M. Solidification in the Direct Metal Deposition by LENS Processing. *JOM* 2001; 53(9): 30–34.
2. Carlton HD, Haboub A, Gallegos GF, et al. Damage Evolution and Failure Mechanisms in Additively Manufactured Stainless Steel. *Mater Sci Eng A* 2016; 651: 406–414.
3. Stucker B, Esplin C and Justin D. An Investigation of LENS®-Deposited Medical-Grade CoCrMo Alloys. In: *Solid Freeform Fabrication Symposium Proceedings*, Austin, TX, 2004, pp. 68-79.
4. Prabhu AW, Vincent T, Chaudhary A, et al. Effect of microstructure and defects on fatigue behaviour of directed energy deposited Ti–6Al–4V. *Sci Technol Weld Joi* 2015; 20(8): 659-669.
5. Gibson I, Rosen WD and Stucker B. *Additive manufacturing technologies*. Vol. 238. New York: Springer, 2010.
6. Griffith ML, Keicher DM, Atwood CL, et al. Free form fabrication of metallic components using Laser Engineered Net Shaping (LENSTM). In: *Proceedings of 7th Solid Freeform Fabricaion Symposium*, Austin, USA,1996, pp. 125–132.

7 Ter Haar GM and Becker TH. Selective Laser Melting Produced Ti-6Al-4V: Post-Process Heat Treatments to Achieve Superior Tensile Properties. *Materials* 2018; 11: 146. (doi:10.3390/ma11010146)

8 Mishurova T, Cabeza S, Artzt K, et al. An Assessment of Subsurface Residual Stress Analysis in SLM Ti-6Al-4V. *Materials* 2017; 10: 348. (doi:10.3390/ma10040348).

9 Knowles C, Becker T and Tait R. The effect of heat treatment on the residual stress levels within direct metal laser sintered Ti-6Al-4V as measured using the hole-drilling strain gauge method. In: *Proceedings of the 13th international Rapid Product Development Association of South Africa (RAPDASA) Conference*, Sun City, South Africa, 2012, pp. 1–10.

10. T. Vilaro, C. Colin, J.D. Bartout, As-fabricated and heat-treated microstructures of the Ti-6Al-4V alloy processed by selective laser melting, Metall. Mater. Trans. A. 42(10) (2011) 3190-3199.
11. Zhai Y, Galarraga H and Lados DA. Microstructure, static properties, and fatigue crack growth mechanisms in Ti-6Al-4V fabricated by additive manufacturing: LENS and EBM. Eng Fail Anal 2016; 69: 3–14.
12. Sterling AJ, Torries B, Shamsaei N, et al. Fatigue behavior and failure mechanisms of direct laser deposited Ti–6Al–4V. Mater Sci Eng A 2016; 655: 100-112.
13. Razavi SMJ, Ferro P, Berto F, et al. Fatigue strength of blunt V-notched specimens produced by selective laser melting of Ti-6Al-4V. Theor Appl Fract Mech (In Press) (DOI: https://doi.org/10.1016/j.tafmec.2017.06.021)
14. Edwards P and Ramulu M. Fatigue performance evaluation of selective laser melted Ti–6Al–4V. *Mater Sci Eng A* 2014; 598: 327–337.
15. Shi X, Ma S, Liu C, et al. Selective laser melting-wire arc additive manufacturing hybrid fabrication of Ti-6Al-4V alloy: Microstructure and mechanical properties. *Mater Sci Eng A* 2017; 684: 196-204.
16. Razavi SMJ, Ferro P and Berto F. Fatigue Assessment of Ti–6Al–4V Circular Notched Specimens Produced by Selective Laser Melting. *Metals* 2017; 7: 291.

17. Qiu C, Adkins NJE and Attallah MM. Microstructure and tensile properties of selectively laser-melted and of HIPed laser-melted Ti–6Al–4V. *Mater Sci Eng A* 2013; 578: 230–239.

18. Razavi SMJ, Bordonaro GG, Ferro P, et al. Fatigue Behavior of Porous Ti-6Al-4V Made by Laser-Engineered Net Shaping. *Materials* 2018; 11(2): 284. (doi:10.3390/ma11020284)

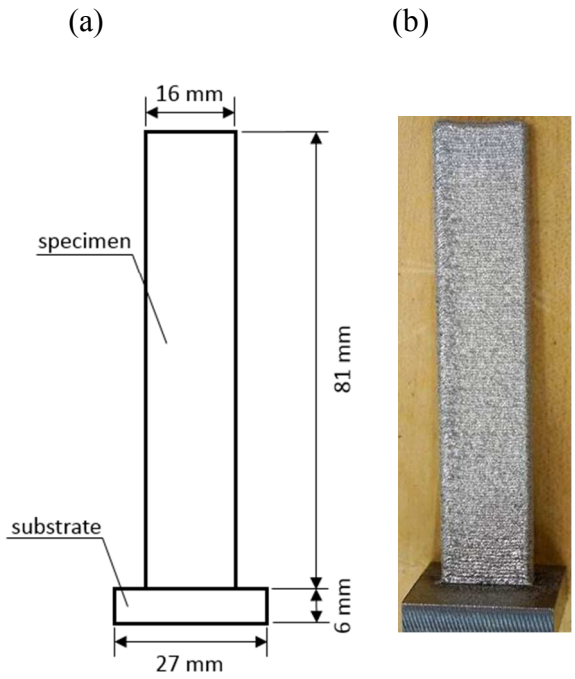

Fig. 1. Dimensioned drawing of the specimen (a), and as-built LENS Ti-6Al-4V sample deposited on the substrate (b).

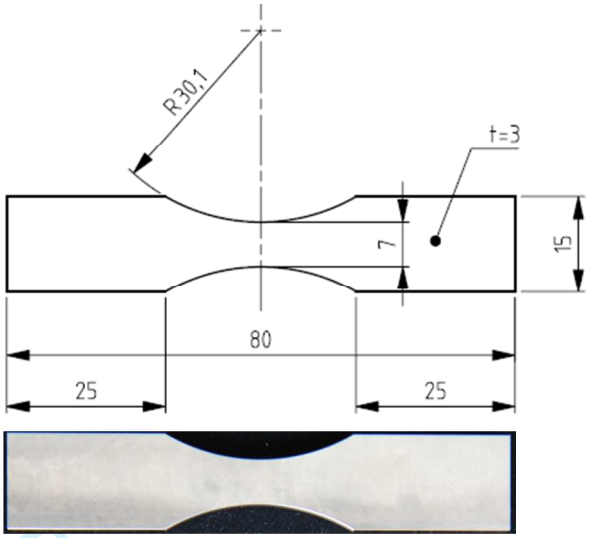

Fig. 2. Dimensions of LENS Ti-6Al-4V specimens.

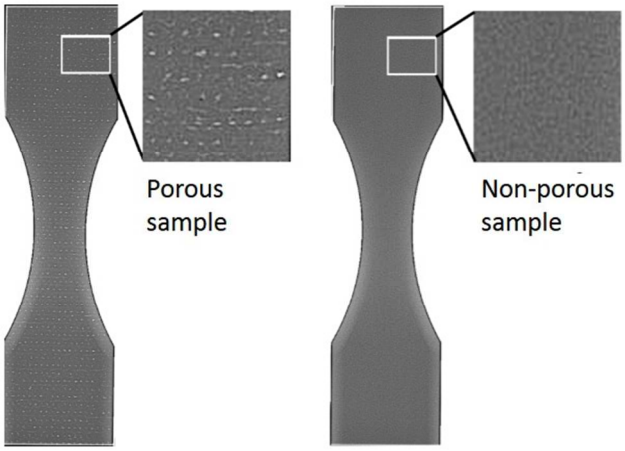

Fig. 3. X-Ray photographs of porous and non-porous samples.

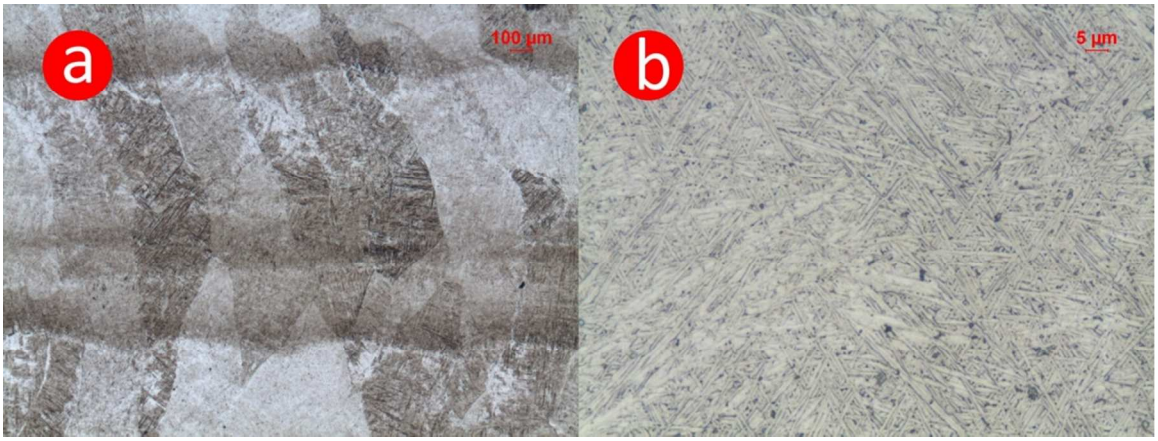

Fig. 4. Columnar prior grains in microstructure section parallel to DED build direction (BD) (a) and acicular α' microstructure (b) of non-porous samples.

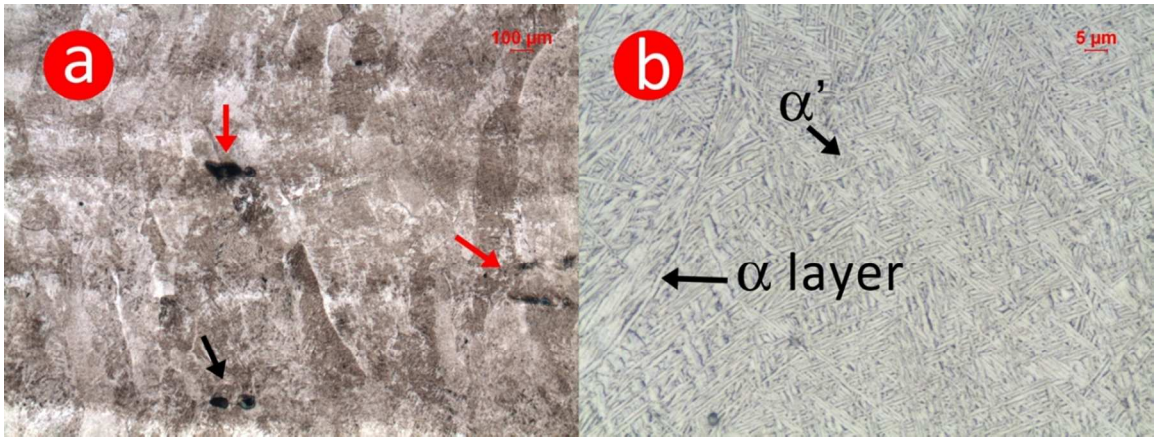

Fig. 5. Columnar prior grains in microstructure section parallel to DED build direction (BD) (a) and acicular α' microstructure (b) of porous samples.

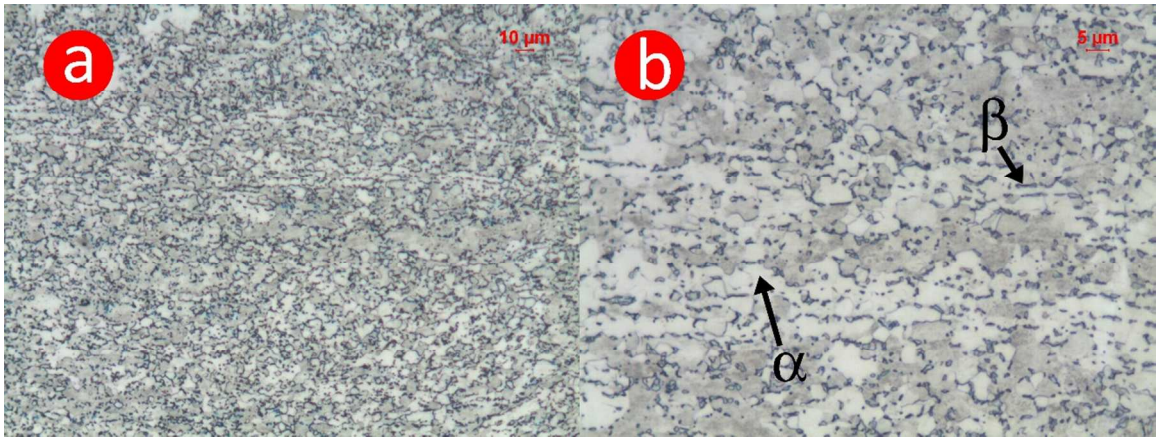

Fig. 6. Microstructure at different magnifications of the wrought Ti-6Al-4V alloy.

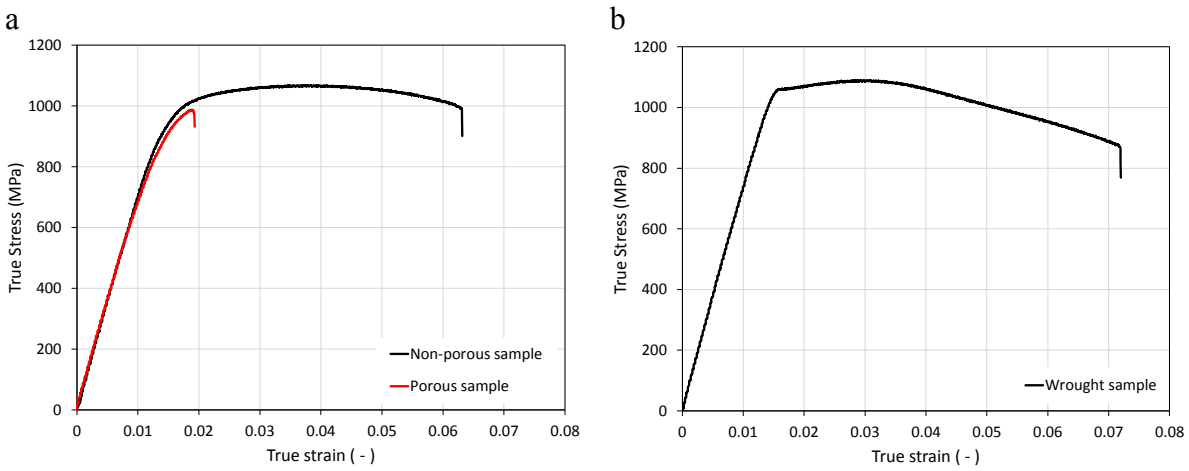

Fig. 7. Tensile properties (stress-strain curves), (a) porous and non-porous samples produced by LENS, (b) wrought samples.

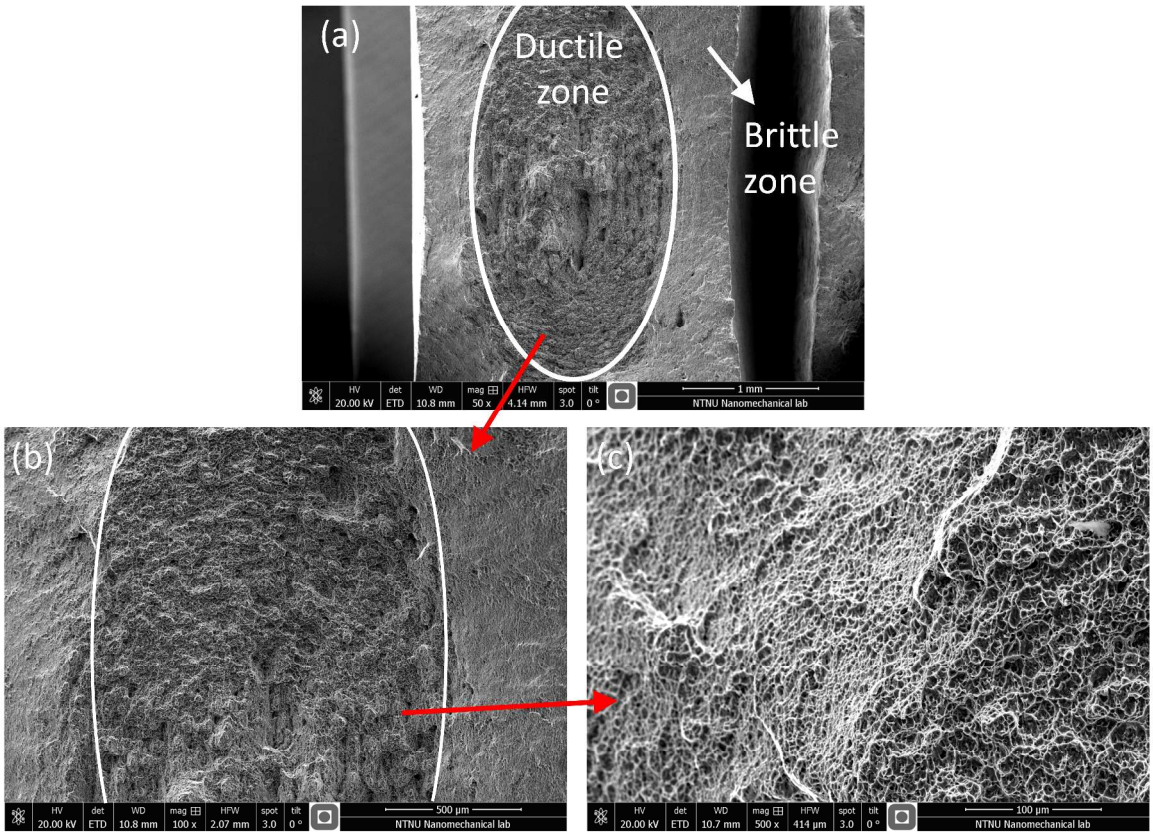

Fig. 8. SEM images of fracture surface of the tested wrought samples.

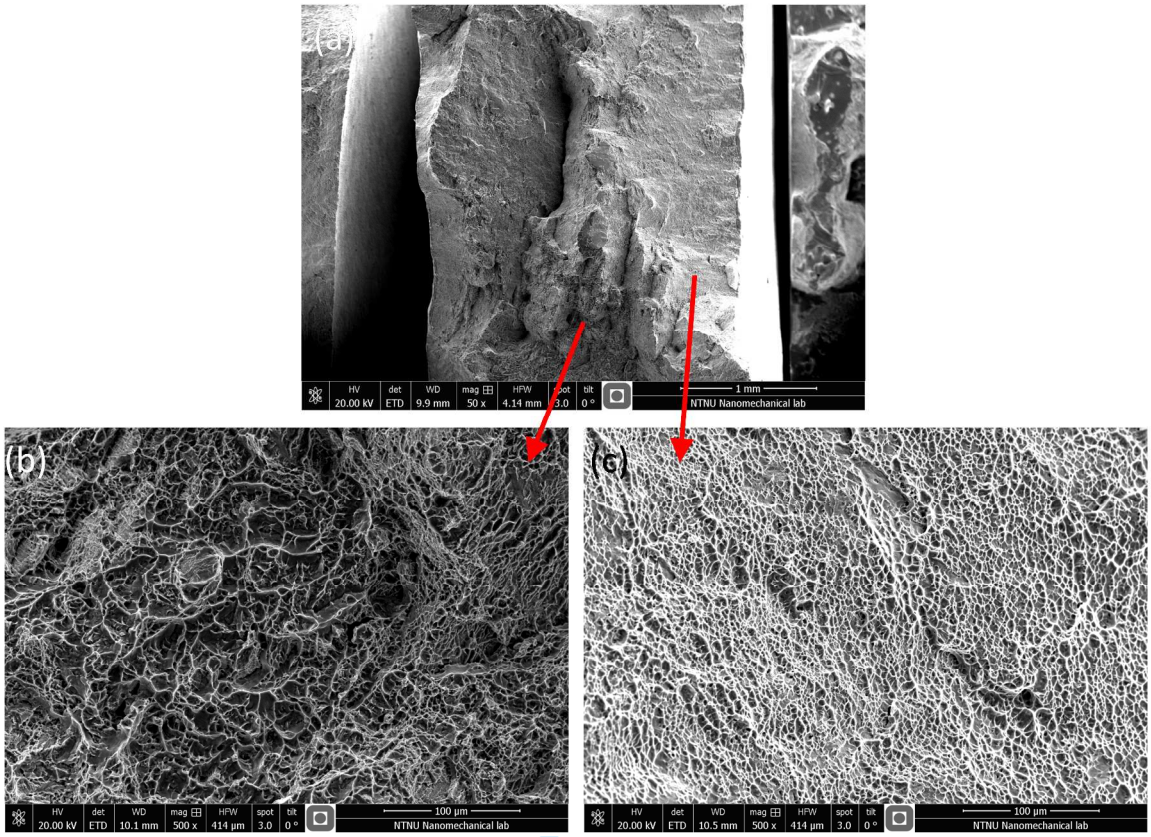

Fig. 9. SEM images of fracture surface of the tested non-porous samples.

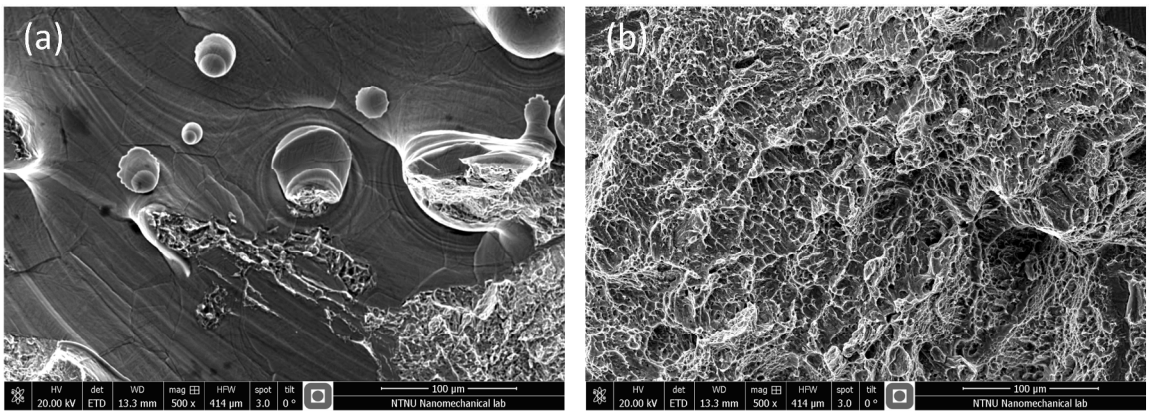

Fig. 10. SEM images of fracture surface of the tested porous samples, (a) porous area, (b) non-porous area.